0026-895X/03/6402-521–532$7.00
MOLECULAR PHARMACOLOGY
Vol. 64, No. 2
2511/1083441
Mol Pharmacol 64:521–532, 2003
Printed in U.S.A.

cGMP/Protein Kinase G-Dependent Potentiation of Glutamatergic Transmission Induced by Nitric Oxide in Immature Rat Rostral Ventrolateral Medulla Neurons in Vitro

CHIUNG-CHUN HUANG, SAMUEL H. H. CHAN, and KUEI-SEN HSU

Department of Pharmacology, College of Medicine, National Cheng Kung University, Tainan, Taiwan (C.C.H., K.S.H.); and Center for Neuroscience, National Sun Yat-sen University, Kaohsiung, Taiwan (S.H.H.C.)

Received March 10, 2003; accepted May 12, 2003

This article is available online at http://molpharm.aspetjournals.org

ABSTRACT

Although both nitric oxide (NO) and glutamate within the rostral ventrolateral medulla (RVLM) are important mediators of the central cardiovascular regulation, little is known about the functional interactions between these two mediators. Herein, we investigated the possible role of NO on the glutamatergic transmission of RVLM neurons. Whole-cell patch-clamp recordings were performed on visualized RVLM neurons in the brainstem slice preparation of rats. We found that bath application of L-arginine, the substrate for NO production, significantly increased the amplitude of excitatory postsynaptic currents (EPSCs). This enhancement was completely abolished by coadministration of the NO synthase inhibitor 7-nitroindazole and mimicked by the NO donors 3-morpholinylsydnoneimine and spermine NONOate. Bath application of a NO-sensitive guanylyl cyclase inhibitor, 1H-[1,2,4]oxadiazolo[4,3-*a*]quinoxalin-1-one, or a protein kinase G (PKG) inhibitor, *R*p-8-bromo-guanosine 3′,5′-cyclic monophosphorothioate, fully prevented the L-arginine-, 3-morpholinylsydnoneimine-, and *N*-[4-[1-(3-aminopropyl)-2-hydroxy-2-nitrosohydrazino]-butyl]-1,3-propanediamine (spermine NONOate)-induced synaptic potentiation. Direct activation of PKG with 8-(4-chlorophenylthio)-cGMP mimicked the action of NO donors. Furthermore, the augmentation by spermine NONOate of EPSC was accompanied by a reduction of the paired-pulse facilitation and synaptic failure rate of EPSCs. Spermine NONOate also significantly increased the frequency of both spontaneous and miniature EPSCs without altering their amplitude distribution. Pretreatment with the N-type Ca^{2+} channel blocker ω-conotoxin GVIA selectively blocked the spermine NONOate-induced synaptic potentiation. These results suggest that NO acts presynaptically to elicit a synaptic potentiation on the RVLM neurons through an enhancement of presynaptic N-type Ca^{2+} channel activity leading to facilitating glutamate release. The presynaptic action of NO is mediated by a cGMP/PKG-coupled signaling pathway.

It is well known that rostral ventrolateral medulla (RVLM) neurons play an important role in cardiovascular, respiratory, and nociceptive functions (Dampney, 1994). Both electrophysiological and anatomical studies showed that a subset of RVLM neurons directly innervates preganglionic vasomotor neurons in the intermediolateral cell columns of the spinal cord, which are involved in the regulation of vasomotor and cardiac tone (Morrison et al., 1991; Deuchars et al., 1995). In addition, the RVLM neurons are tonically active in vivo and receive convergent excitatory and inhibitory inputs from multiple sources (Mtui et al., 1995; Guyenet et al., 1996). However, little is known regarding the physiological regulation of the tonic excitation of these neurons.

Nitric oxide (NO), an unstable diatomic radical synthesized from L-arginine by nitric-oxide synthase (NOS), is recognized as an important signaling molecule mediating a variety of physiological processes, including synaptic transmission and synaptic plasticity (Garthwaite, 1991). In addition, considerable evidence suggests that NO is also involved in central cardiovascular regulation and that one of the potential sites in the central nervous system for NO to exert its modulation action on cardiovascular functions is the

This work was supported in part by the Academic Excellence Program (grant 89-B-FA08-1-4 to K.S.H., S.H.H.C.) from the Ministry of Education, Taiwan.

ABBREVIATIONS: RVLM, rostral ventrolateral medulla; NO, nitric oxide; NOS, nitric-oxide synthase; iNOS, inducible nitric-oxide synthase; nNOS, neuronal nitric-oxide synthase; sGC, soluble guanylyl cyclase; PKG, cGMP-dependent protein kinase; ACSF, artificial cerebrospinal fluid; EPSC, excitatory postsynaptic current; sEPSC, spontaneous excitatory postsynaptic current; QX-314, lidocaine *N*-ethyl bromide; mEPSC, miniature excitatory postsynaptic current; 7-NI, 7-nitroindazole; ODQ, 1H-[1,2,4]oxadiazolo[4,3-*a*]quinoxalin-1-one; SIN-1, 3-morpholinylsydnoneimine; CNQX, 6-cyano-7-notroquinoxaline-2,3-dione; spermine NONOate, *N*-[4-[1-(3-aminopropyl)-2-hydroxy-2-nitrosohydrazino]-butyl]-1,3-propanediamine; D-APV, D-(−)-α-amino-5-phosphonopentanoic acid; TTX, tetrodotoxin; *R*p-8-Br-cGMPS, Rp-8-bromo-guanosine 3′,5′-cyclic monophosphorothioate; 8-pCPT-cGMP, 8-(4-chlorophenylthio)-guanosine-3′,5′-cyclic monophosphate; PPF, paired-pulse facilitation; ω-Aga-TK, ω-agatoxin-TK.

RVLM (Hakim et al., 1995; Zanzinger et al., 1995; Hirooka et al., 1996; Kagiyama et al., 1997; Chan et al., 2001). Studies using immunohistochemistry, NADPH-diaphorase staining, or autoradiography further demonstrate the presence of neuronal NOS (nNOS), inducible NOS (iNOS), and endothelial NOS in the RVLM (Vincent and Kimura, 1992; Chang et al., 2001). We demonstrated recently (Chan et al., 2001) that both nNOS and iNOS in the RVLM are tonically active under physiological conditions at the levels of functional expression and molecular synthesis. More importantly, we showed that the prevalence of nNOS over iNOS activity at the RVLM and the associated dominance of sympathoexcitation over sympathoinhibition underlie the maintenance of sympathetic vasomotor outflow and stable arterial pressure by the endogenous NO.

An important corollary to these findings is how NO exerts its modulatory action on RVLM neurons to regulate the cardiovascular function. Because glutamate is the major neurotransmitter in tonic excitatory drive of RVLM neurons (Sved et al., 2001), we have therefore examined the role of NO on the glutamatergic transmission of RVLM neurons in brainstem slice preparations from immature rats using whole-cell patch-clamp recordings. Our results suggest that NO acts presynaptically to elicit a stable potentiation of synaptic transmission by means of a mechanism involving the NO-sensitive sGC/cGMP/PKG-coupled signaling cascade, and these effects may have resulted in a sympathoexcitatory effect of NO in the RVLM.

Materials and Methods

Slice Preparation. Animal care was consistent with the guidelines set by the Laboratory Animal Center of National Cheng Kung University. All experimental procedures were approved by the NCKU Institutional Animal Use and Care Committee. Coronal brainstem slices containing RVLM were prepared from immature (7- to 9-day-old) male Sprague-Dawley rats for whole-cell patch-clamp recordings by procedures described previously (Hwang and Dun, 1998). In brief, rats were killed by decapitation under halothane anesthesia, and coronal brainstem slices (200 μm thick) were prepared using a vibrating microtome (Leica VT1000S; Leica, Nussloch, Germany). The slices were placed in a storage chamber of artificial cerebrospinal fluid (ACSF) oxygenated with 95% O_2/5% CO_2 and kept at room temperature for at least 1 h before recording. The composition of the ACSF solution was 117 mM NaCl, 4.7 mM KCl, 2.5 mM $CaCl_2$, 1.2 mM $MgCl_2$, 25 mM $NaHCO_3$, 1.2 mM NaH_2PO_4, and 11 mM glucose at pH 7.3 to 7.4 and equilibrated with 95% O_2/5% CO_2.

Patch-Clamp Recordings. For patch-clamp recording, slices were transferred to a recording chamber and fixed at the glass bottom of the chamber with a nylon grid on a platinum frame. The chamber consisted of a circular well of a low volume (1–2 ml) and was perfused constantly at room temperature (24–26°C) at a speed of 2 to 3 ml/min. Visualized whole-cell patch-clamp recordings of synaptically evoked EPSCs and spontaneous EPSCs (sEPSCs) were conducted using standard methods (Huang et al., 2001). The RVLM was recognized in the slice as an area ventral to the nucleus ambiguous that appears as a slightly dark area in a freshly prepared medullary slice and lateral to the paragigantocellular nucleus at a level rostral to the area postrema (Hwang and Dun, 1998). The RVLM neurons were visualized throughout the experiment with an upright microscope (BX50WI; Olympus, Tokyo, Japan) equipped with a water-immersion 40× objective using Nomarski-type differential interference contrast optics combined with infrared videomicroscopy. Patch pipettes were pulled from borosilicate capillary tubing and heat polished. The electrode resistance was typically 4 to 5 MΩ. The composition of intracellular solution was 115 mM K-gluconate, 20 mM KCl, 10 mM HEPES, 2 mM $MgCl_2$, 10 mM EGTA, 3 mM Na_2ATP, 0.3 mM Na_3GTP, 5 mM QX-314, and sucrose to bring osmolarity to 290 to 295 mOsM and pH to 7.3. After a high resistance seal (> 2 GΩ before breaking into whole-cell mode) was obtained, suction was applied lightly through the pipette to break through the membrane. The cell was then maintained at −70 mV for several minutes to allow diffusion of the internal solution into the cell body and dendrites. Recordings were made using an Axopatch 200B (Axon Instruments, Union City, CA) amplifier. Electrical signals were low-pass filtered at 2 kHz and digitized at 4 to 10 kHz using a Digidata 1200B interface. An Intel Pentium-based computer with pCLAMP software (version 8.0; Axon Instruments) was used for on-line acquisition and off-line analysis of the data. For measurement of synaptically evoked EPSCs, a bipolar stainless steel stimulating electrode was applied to a site 300 to 450 μm dorsal to the recorded neurons; the superfusate routinely contained bicuculline methiodide (10 μM) and strychnine hydrochloride (0.5 μM) to block inhibitory synaptic responses. The strength of synaptic transmission was quantified by measuring the amplitude of EPSCs over a 0.5- to 2-ms window concentrated around the peak. Series resistance (Rs) was calculated according to Rs = 10 mV/I, where I was the peak of transient current (filtered with 10 kHz) evoked by the 10-mV testing pulse when the pipette capacitance was compensated fully. Only cells demonstrating <25 MΩ series resistance (usually 10–20 MΩ) were used in these experiments.

sEPSCs comprise both action potential-dependent and -independent synaptic events observed in the absence of synaptic stimulation. In the present study, sEPSCs were recorded from RVLM neurons held in voltage clamp at a potential of −70 mV in the presence of bicuculline methiodide (10 μM) and strychnine hydrochloride (0.5 μM) and analyzed off-line using a commercially available software (Mini Analysis 4.3; Synaptosoft, Leonia, NJ). The software detects events based on amplitudes exceeding a threshold set just above the baseline noise of the recording. The threshold for detection was set at −3 pA. All detected events were re-examined and accepted or rejected based on subjective visual examination. The program then measured amplitudes and intervals between successive detected events. Frequencies were calculated by dividing the total number of detected events by the total time sampled. Periods of 5 to 10 min were analyzed for each pharmacological treatment, and these recordings were visually inspected to allow for the removal of artifacts. Cumulative probability plots were constructed to compare drug effects on the distribution of amplitude and interevent intervals from sEPSCs. Amplitude histograms were binned in 1-pA intervals.

Drug Application. All drugs were applied by dissolving them to the desired final concentrations in the ACSF and by switching the perfusion from control ACSF to drug-containing ACSF. Appropriate stock solutions of drugs were made and diluted with ACSF just before application. 7-NI, nimodipine, and ODQ were dissolved in dimethyl sulfoxide stock solutions and stored at −20°C until the day of experiment. Other drugs used in this study were dissolved in distilled water. The concentration of DMSO in the perfusion medium was 0.1%, which alone had no effect on the basal synaptic transmission. L-Arginine, 7-NI, ODQ, SIN-1, nimodipine, ω-conotoxin GVIA, 6-cyano-7-notroquinoxaline-2,3-dione (CNQX), spermine NONOate, D-(−)-α-amino-5-phosphonopentanoic acid (D-APV), and bicuculline methiodide were purchased from Tocris Cookson (Bristol, UK); D-arginine, strychnine hydrochloride, and tetrodotoxin (TTX) were obtained from Sigma (St. Louis, MO); *R*p-8-Br-cGMPS and 8-pCPT-cGMP were purchased from Calbiochem (La Jolla, CA). ω-Agatoxin TK was obtained from Almone (Jerusalem, Israel).

Statistical Analysis. The data for each experiment were normalized relative to baseline and are presented as means ± S.E.M. *n* indicates the number of experiments. The significance of the difference between the mean was calcu-

lated by paired or unpaired Student's t test. Probability values (p) of less than 0.05 were considered to represent significant differences. Comparisons between control and experimental distributions of sEPSC amplitude and interevent intervals were made by performing Kolmogorov-Smirnov test. Distributions were considered different using a conservative critical probability level of $p < 0.01$.

Results

Whole-cell patch-clamp recordings were made from neurons in the RVLM area. The RVLM was recognized in the slice as an area ventral to the compact region of nucleus ambiguous, which appeared as a slightly dark area in the freshly prepared slice, lateral to the paragigantocellular nucleus at the level rostral to area postrema, as shown in Fig. 1A. Other than the general location, RVLM neurons were not further characterized with respect to their transmitter phenotype or functional identity. All RVLM neurons included in this study had a longitudinal diameter of the soma ranging from 12 to 16 μm, and their perikarya were rhombic, fusiform, or triangular in shape (Fig. 1B). These neurons had a mean resting membrane potential, spike height, and input resistance of -61.2 ± 2.8 mV, 72.3 ± 2.9 mV, and 632 ± 68 MΩ ($n = 32$), respectively, which are comparable with the values reported previously (Hwang and Dun, 1998). In all experiments, neurons were clamped at -70 mV and EPSCs were evoked by intra-RVLM stimulation with bipolar stimulating electrode every 20 s in the presence of the $GABA_A$ receptor antagonist bicuculline methiodide (10 μM) and the glycine receptor antagonist strychnine hydrochloride (0.5 μM).

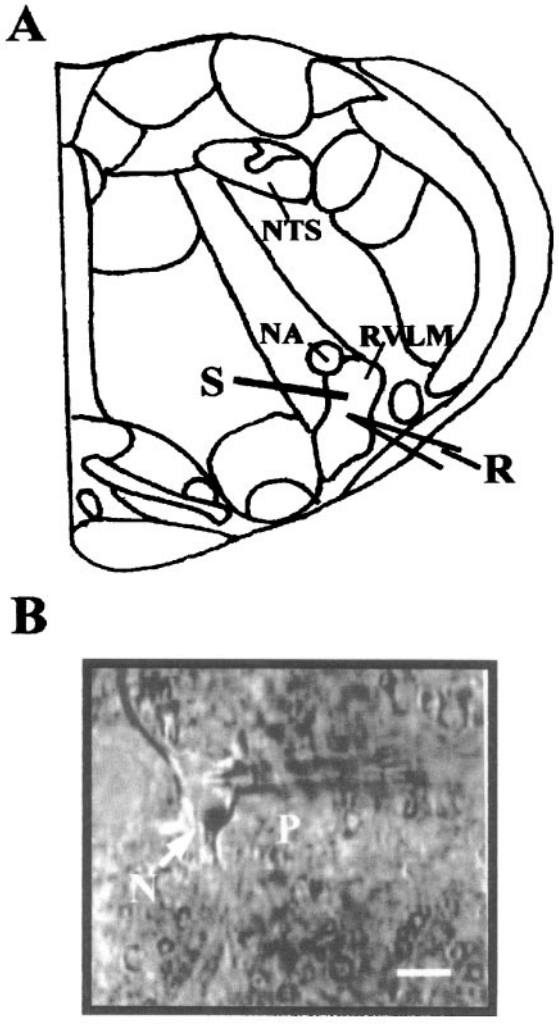

Fig. 1. Visual identification of the recorded neurons in the RVLM. A, diagram of a coronal brainstem slice illustrating electrical stimulation (S) and patch recording (R) sites. NTS, nucleus tractus solitarii; NA, nucleus ambiguous. B, an infrared microscope image of a RVLM neuron (N) in a slice from an 8-day-old rat. The patch recording pipette (P) can be seen on the right. Calibration bar, 15 μm.

Exogenous NO-Induced Synaptic Potentiation. We examined initially the effect of L-arginine, the substrate for NO production by NOS, on the evoked EPSCs. In six of eight cells tested, bath application of 200 μM L-arginine for 10 min produced a significant enhancement of evoked EPSCs. The mean EPSC amplitude after L-arginine was increased by $24.9 \pm 5.8\%$ of the control baseline ($n = 8$; $p < 0.05$; paired Student's t test) (Fig. 2, A and C). The EPSCs recovered toward the control level within a few minutes after washout of L-arginine, suggesting the reversibility of L-arginine effect. At the end of each experiment, the non-NMDA receptor antagonist CNQX (20 μM) and NMDA receptor antagonist D-APV (50 μM) were added to the bath to ensure that the synaptic response was glutamatergic EPSC. In the same concentration, D-arginine did not cause a significant change of EPSCs ($4.5 \pm 2.3\%$ of the control baseline, $n = 4$; $p > 0.05$; paired Student's t test) (Fig. 2C).

To confirm that L-arginine-induced synaptic potentiation is caused by the synthesis of NO, we tested the effects of blocking nNOS. As shown in Fig. 2, B and C, the increase in the amplitude of EPSCs by L-arginine (200 μM) was completely prevented when 7-NI (100 μM), a selective nNOS inhibitor, was preperfused for more than 10 min before L-arginine application ($n = 7$; $p < 0.05$; unpaired Student's t test). In the presence of 7-NI, L-arginine increased the amplitude of EPSCs by a mean of $3.1 \pm 1.7\%$ of pre–L-arginine level. Additionally, bath application of 7-NI (100 μM) alone had a slight but not significant increase in the amplitude of EPSCs ($7.5 \pm 3.8\%$ of the control baseline, $n = 7$; $p > 0.05$; paired Student's t test). These results suggest that the facilitating action of L-arginine on glutamatergic transmission on the RVLM neurons is mediated by the nNOS-mediated synthesis of NO.

Additional evidence that NO can induce a synaptic potentiation of glutamatergic transmission on the RVLM neurons came from experiments using the NO donors SIN-1 and spermine NONOate. Similar to L-arginine, bath application for 10 min of the SIN-1 (200 μM) or spermine NONOate (100 μM) produced a significant enhancement in six of eight and six of eight cells tested, respectively. The mean EPSC amplitude after SIN-1 or spermine NONOate was 24.9 ± 4.4 and $22.5 \pm 4.3\%$ of the control baseline, respectively ($n = 8$ and 8; $p < 0.05$; paired Student's t test) (Fig. 3).

NO Enhances Synaptic Transmission through a sGC/cGMP/PKG-Coupled Signaling Pathway. An established signal transduction pathway for NO is activation of sGC, leading to an increase in intracellular cGMP levels (Ignarro, 1991). Thus, to address the involvement of cGMP in the action of NO on glutamatergic transmission on the RVLM neurons, we investigated whether the pharmacological inhibition of sGC was able to prevent the synaptic potentiation caused by L-arginine and NO donors. Preincubation of the

slices with 10 μM ODQ, a selective inhibitor of sGC, caused no change in the amplitude of EPSCs (107.6 ± 4.6% of the control baseline; $n = 15$; $p > 0.05$; paired Student's t test) but fully blocked the synaptic potentiation caused by L-arginine, SIN-1, and spermine NONOate (Fig. 4). In the presence of ODQ (10 μM), bath application of L-arginine (200 μM), SIN-1 (200 μM), or spermine NONOate (100 μM) for 10 min produced only a minor increase in the amplitude of EPSCs by 12.5 ± 3.2% ($n = 5$), 9.5 ± 3.6% ($n = 5$), and 5.3 ± 3.5% ($n = 5$), respectively, which were significantly different from those produced by L-arginine, SIN-1, or spermine NONOate alone ($p < 0.05$; unpaired Student's t test).

Intracellular elevation of cGMP levels may result in the stimulation of PKG, which in turn modulates the function of a series of cellular substrates by increasing their phosphorylation state. To examine the role of PKG in the action of NO on glutamatergic transmission on the RVLM neurons, the effect of a selective PKG inhibitor, *R*p-8-Br-cGMPS, on SIN-1- and spermine NONOate-induced synaptic potentiation was investigated. In these experiments, slices were incubated for at least 1 h in 50 μM *R*p-8-Br-cGMPS before being transferred to the recording chamber, where the concentration was maintained at 10 μM. Pretreatment of the

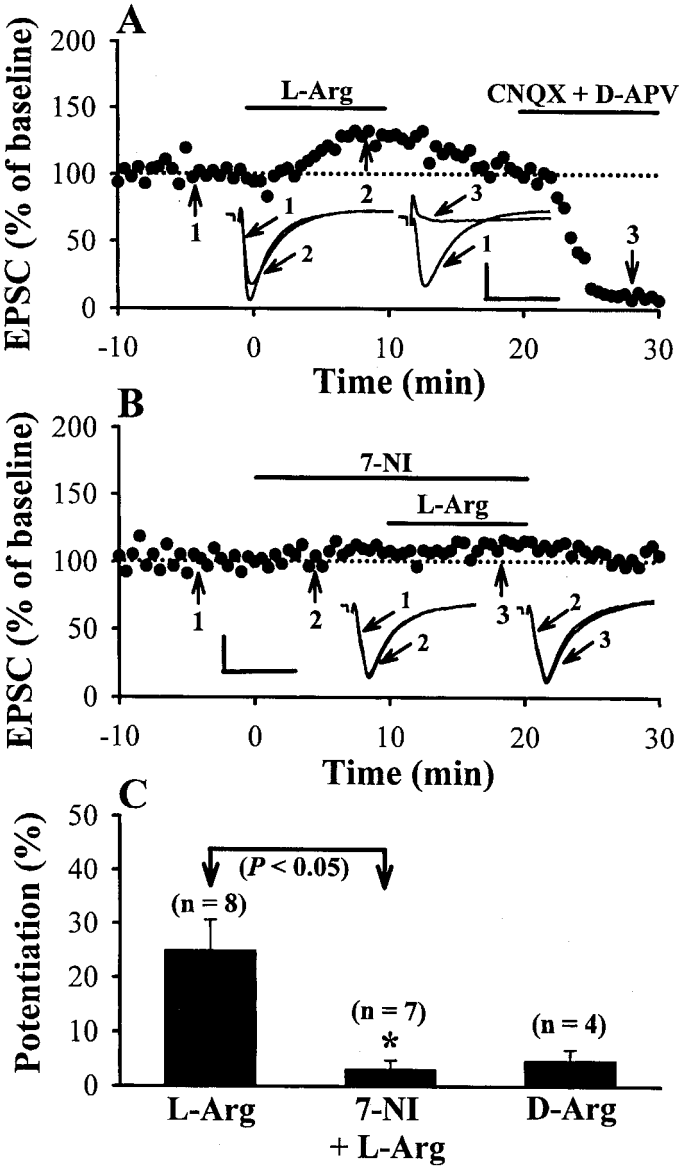

Fig. 2. L-Arginine but not D-arginine enhances synaptically evoked EPSCs on the RVLM neurons. A, a representative experiment showing time course of the action of L-arginine on the peak amplitude of evoked EPSCs. EPSCs were evoked every 20 s by a single pulse and were recorded from a holding potential of −70 mV. Each data point represents a single response evoked before, during, and after the application of 200 μM L-arginine on a RVLM neuron. L-Arginine dramatically enhanced EPSCs, and this effect was reversible on washout for 10 min. At the end of experiment, CNQX (20 μM) and D-APV (50 μM) were applied to the bath to make sure that synaptic response was a glutamatergic EPSC. B, a representative experiment showing that prior application of nNOS inhibitor 7-NI (100 μM) completely prevented the potentiation of EPSCs by L-arginine (200 μM). C, summary histogram showing average percentage potentiation of the amplitude of EPSCs by L-arginine (200 μM) in the control group or in the presence of 7-NI, and D-arginine (200 μM). The superimposed EPSC in the inset of each graph illustrates respective recordings from example experiments taken at the times indicated. Horizontal bars denote the period of delivery of L-arginine or 7-NI. Calibration bars: vertical, 50 pA; horizontal, 20 ms. *, $p < 0.05$; Student's unpaired t test.

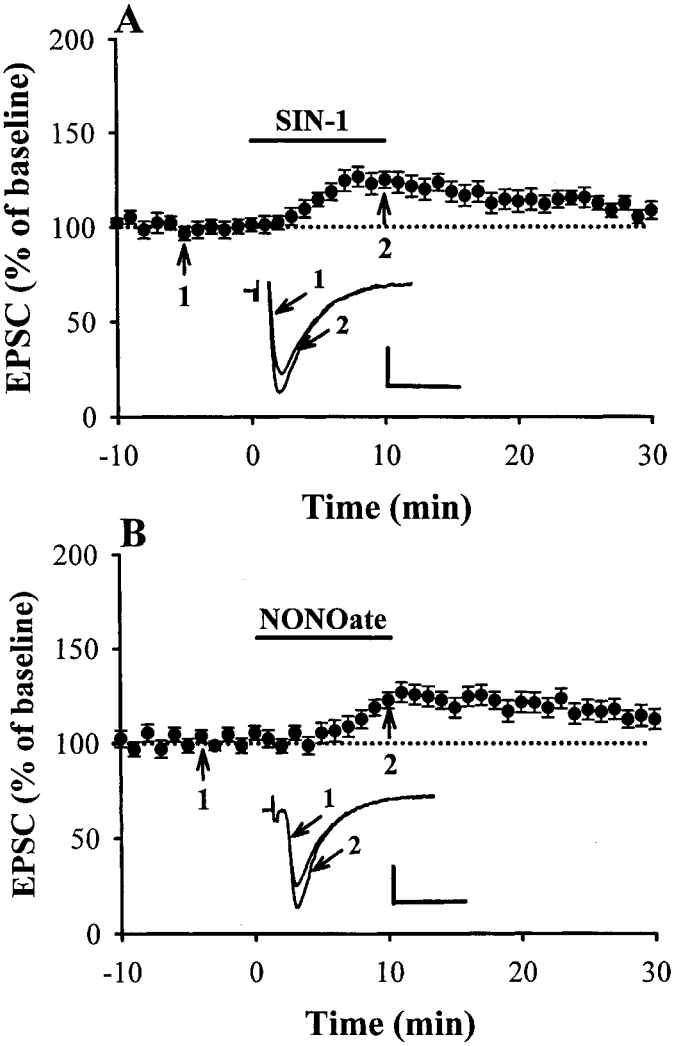

Fig. 3. Effects of SIN-1 and spermine NONOate on evoked EPSCs. A, summary of experiments ($n = 8$) showing that bath application of SIN-1 (200 μM) reversibly increased the amplitude of EPSCs. B, summary of experiments ($n = 8$) showing that application of spermine NONOate (100 μM) also significantly increased the amplitude of EPSCs. The superimposed EPSC in the inset of each graph illustrates respective recordings from example experiments taken at the times indicated. Horizontal bars denote the period of delivery of SIN-1 or spermine NONOate. Calibration bars: vertical, 50 pA; horizontal, 20 ms.

slices with *R*p-8-Br-cGMPS completely blocked the SIN-1- and spermine NONOate-induced synaptic potentiation (Fig. 5, A and B). In the presence of *R*p-8-Br-cGMPS, bath application of SIN-1 (200 μM) or spermine NONOate (100 μM) for 10 min produced only a minor increase in the EPSC amplitude by a mean of 6.5 $\pm$ 3.7 (n = 5) and 10.3 $\pm$ 5.9 (n = 5), respectively, which were significantly different from those produced by SIN-1 or spermine NONOate alone ($p < 0.05$; unpaired Student's t test). To further examine the role of cGMP in synaptic potentiation on the RVLM neurons, we examined the effect of a membrane-permeable cGMP analog, 8-pCPT-cGMP. As shown in Fig. 5C, in six of seven cells tested, bath application of 8-pCPT-cGMP (50 μM) for 20 min mimicked the facilitating action of L-arginine and NO donors. The mean EPSC amplitude after 8-pCPT-cGMP was increased by 24.5 $\pm$ 4.3% of the control baseline (n = 7; $p <$ 0.05; paired Student's t test). These results suggest that NO-induced synaptic potentiation via a mechanism that is triggered by the activation of the sGC/cGMP/PKG-coupled signaling cascade.

Presynaptic Expression of Spermine NONOate-Induced Synaptic Potentiation. Because SIN-1 is now

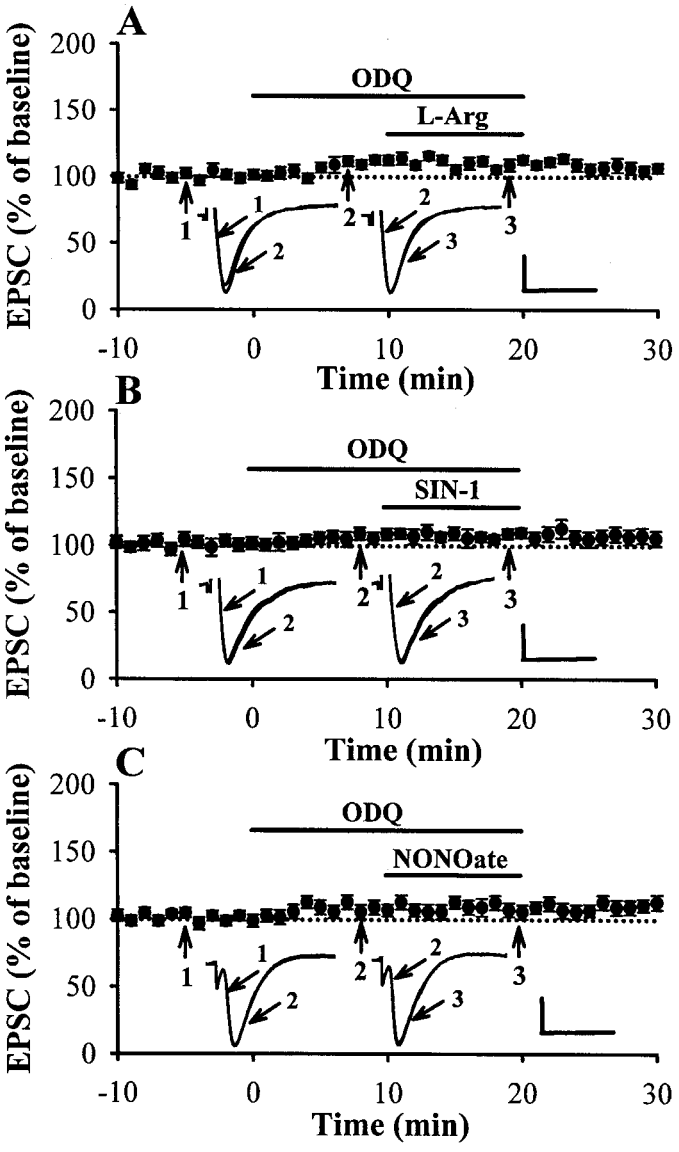

Fig. 4. L-Arginine-, SIN-1, and spermine NONOate-induced increase in the amplitude of EPSCs were completely prevented by ODQ. A, summary of experiments (n = 5) showing that prior application of ODQ (10 μM) completely prevented the potentiation of EPSCs by L-arginine (200 μM). B, summary of experiments (n = 5) showing that SIN-1 (200 μM)-induced synaptic potentiation was completely prevented by prior application of ODQ (10 μM). C, summary of experiments (n = 5) showing that spermine NONOate (100 μM)-induced synaptic potentiation was completely prevented by prior application of ODQ (10 μM). The superimposed EPSC in the inset of each graph illustrates respective recordings from example experiments taken at the time indicated. Horizontal bars denote the period of delivery of drugs as indicated. Calibration bars for: vertical, 50 pA; horizontal, 20 ms.

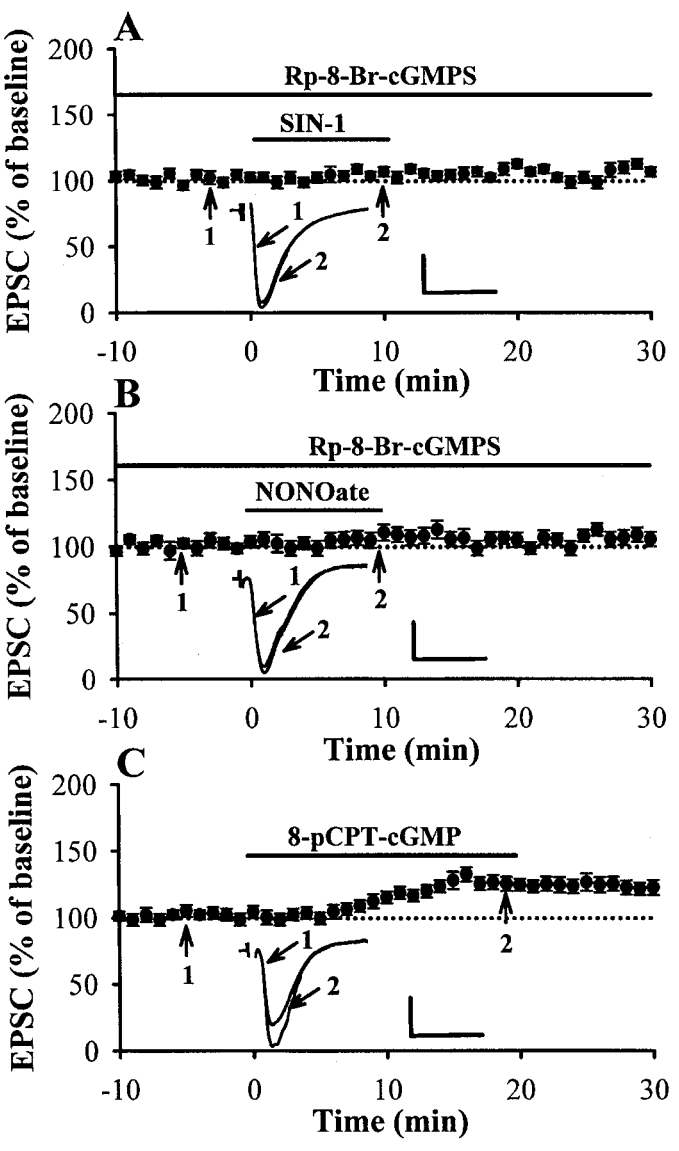

Fig. 5. Role of PKG in the SIN-1- and spermine NONOate-induced increase in the amplitude of EPSCs. A, summary of experiments (n = 5) showing that pretreatment of the slices with *R*p-8-Br-cGMPS (10 μM), an inhibitor of PKG, fully prevented the potentiation of EPSCs by SIN-1 (200 μM). B, summary of experiments (n = 5) showing that spermine NONOate (100 μM)-induced synaptic potentiation was completely prevented by pretreatment of the slices with *R*p-8-Br-cGMPS (10 μM). C, summary of experiments (n = 7) showing that bath application of 8-pCPT-cGMP (50 μM) mimicked SIN-1 and spermine NONOate-induced synaptic potentiation. The superimposed EPSC in the inset of each graph illustrates respective recordings from example experiments taken at the times indicated. Horizontal bars denote the period of delivery of drugs as indicated. Calibration bars: vertical, 50 pA; horizontal, 20 ms.

known to have other effects related to its ability to produce peroxynitrite, we therefore used only spermine NONOate to investigate the further mechanisms underlying the NO-induced synaptic potentiation on the RVLM neurons (Holm et al., 1998; Trackey et al., 2001). To identify whether the NO action was on presynaptic or postsynaptic sites, two different approaches were used. We initially addressed this issue by examining the effect of spermine NONOate on the failure rate of single-fiber EPSCs evoked by minimal stimulation, which reflects changes in the presynaptic transmitter release (Stevens and Wang, 1994; Raastad, 1995). As a typical example shown in Fig. 6A, the expression of spermine NONOate-induced synaptic potentiation is accompanied by a decrease in the synaptic failure rate. On average, the failure rate was decreased from 62.4 ± 3.4% to 34.2 ± 2.6% after spermine NONOate (100 μM) application ($n = 5$; $p < 0.05$; paired Student's t test) (Fig. 6B).

To further test the possibility that spermine NONOate-induced synaptic potentiation through a presynaptic mechanism, we conducted studies examining the effects of spermine NONOate on PPF. When the excitatory afferents to the central neurons are activated twice with a short interval between each stimulus, the response to the second stimulus is generally facilitated in relation to the initial stimulus. This phenomenon is called a PPF and is attributed to an increase the amount of transmitter release to the second stimulus (Zucker, 1989). On the other hand, the manipulations of presynaptic transmitter release may result in the change in the magnitude of PPF. If the spermine NONOate-induced synaptic potentiation involved a presynaptic mechanism of action, it will be associated with a change in the magnitude of PPF. Alternatively, if spermine NONOate induced synaptic modulation by another type of mechanism (e.g., reducing the sensitivity of postsynaptic receptors), then the PPF magnitude should be relatively unaffected. To test this hypothesis, the magnitude of PPF was determined at control before the application of spermine NONOate and 10 min after starting the application of spermine NONOate. Figure 6C shows a typical example of EPSCs synaptically evoked in response to a pair of stimuli with an interpulse interval of 30 ms. We found that the increase of the amplitude of EPSCs induced by spermine NONOate (100 μM) was accompanied by a decrease in the magnitude of PPF. The magnitude of PPF was 2.29 ± 0.18% before and 1.67 ± 0.11% ($n = 5$; $p < 0.05$; paired Student's t test) during the application of spermine NONOate. These results suggest that NO may act presynaptic site to modulate the transmitter release mechanisms in the RVLM.

Effects of NO on Spontaneous Excitatory Postsynaptic Currents. To further confirm the possibility that NO modulates the evoked EPSCs through a presynaptic mechanism, we examined the effects of spermine NONOate on sEPSCs. sEPSCs in the RVLM neurons were measured under voltage clamp at −70 mV and were pharmacologically isolated from spontaneous inhibitory currents by the inclusion of 10 μM bicuculline methiodide and 0.5 μM strychnine hydrochloride in the ACSF perfusing the slices. The sEPSCs were totally blocked by bath coapplication of CNQX (20 μM)

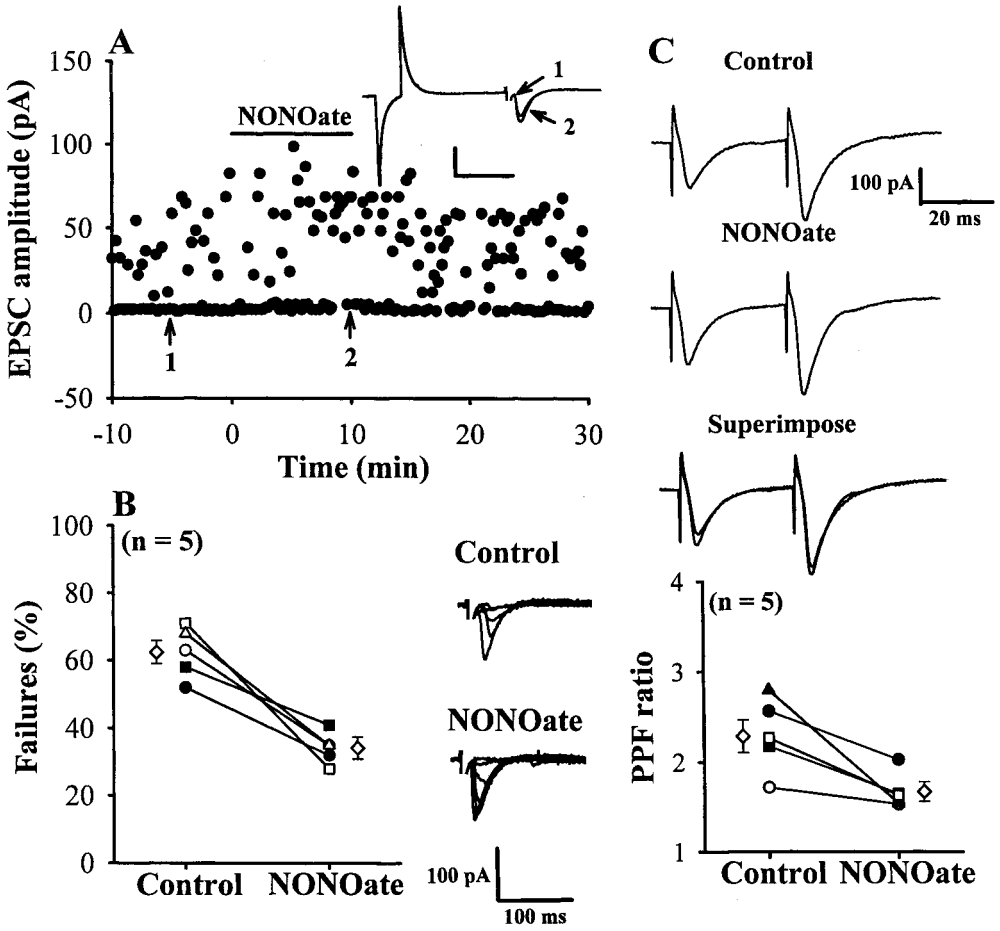

Fig. 6. Failure and PPF analysis of spermine NONOate-induced synaptic potentiation. A, plot of EPSC amplitude recorded at −70 mV holding potential against time, before and after bath application of spermine NONOate (100 μM) for 10 min, evoked at 0.1 Hz by minimal stimulation. It is clear that spermine NONOate produced a significant decrease in the number of failures. Sample traces are averages of six consecutive EPSCs recorded at the times indicated by the numbers on the graph. Calibration: 100 pA, 20 ms. B, summary of five experiments comparing the failure rate before and after spermine NONOate application. Superimposed EPSC traces from a representative experiment show baseline transmission (Control) and the decrease in failure rate after application of spermine NONOate. C, effects of spermine NONOate (100 μM) on the PPF ratio calculated from the responses to paired-pulse stimulation with an interpulse interval of 30 ms. PPF ratio was defined as (p2/p1) × 100%, where p1 and p2 are the amplitude of the EPSCs evoked by the first and second pulses, respectively. C, top, sample traces showing PPF before and after application of spermine NONOate. C, bottom, summary of experiments ($n = 5$) showing that spermine NONOate (100 μM)-induced synaptic potentiation was accompanied by a decrease in the magnitude of PPF ratio.

and D-APV (50 μM), confirming them to be true glutamate receptor-mediated events. Under control conditions, sEPSCs had a mean amplitude of 6.92 ± 0.33 pA and a variable frequency ranging from 1.0 to 1.6 Hz (mean, 1.32 ± 0.12 Hz; $n = 5$). In five cells tested, spermine NONOate (100 μM) markedly increased the mean frequency of the sEPSCs from 1.32 ± 0.12 to 2.53 ± 0.28 Hz ($p < 0.05$; paired Student's t test) (Fig. 7, A and E). Significant differences in cumulative interevent interval distributions were observed in all five cells tested during spermine NONOate application; i.e., spermine NONOate shifted the interevent interval distribution of sEPSCs to shorter intervals ($p < 0.001$; Kolmogorov-Smirnov test). A typical example of recorded cell is shown in Fig. 7C. However, there was no significant effect of spermine NONOate (100 μM) on the sEPSC amplitude. This can be observed by a lack of effect of spermine NONOate on either the amplitude histogram (Fig. 7B) or the cumulative probability plots (Fig. 7B, inset; $p = 0.54$; Kolmogorov-Smirnov test). The mean amplitude of sEPSCs recorded in the presence of spermine NONOate (100 μM) was 8.08 ± 0.56 pA, which was of comparable amplitude with that of sEPSCs recorded under control conditions (6.92 ± 0.33 pA; $p > 0.05$; paired Student's t test).

The spontaneous synaptic events recorded from the RVLM neurons could be roughly divided into two components: TTX-sensitive, action potential-dependent sEPSCs and TTX-resistant, action potential-independent miniature EPSCs (mEPSCs). The action potential-dependent sEPSCs arise from presynaptic impulses, whereas the action potential-independent mEPSCs are thought to result from spontaneous fusion of neurotransmitter-containing vesicles to the presynaptic terminal membrane in a manner independent of the activation of presynaptic voltage-dependent ion channels. We next examined the effect of spermine NONOate on mEPSCs to determine whether NO can modulate action potential-independent spontaneous events. TTX (1 μM) was added to the perfusate in the presence of bicuculline methiodide and strychnine hydrochloride to eliminate sEPSCs arising from presynaptic impulses. In all cells recorded, the efficacy of TTX block of Na^+ channels was monitored by observing the disappearance of the evoked EPSCs during maximal electrical stimulation (data not shown). Application of TTX (1 μM)

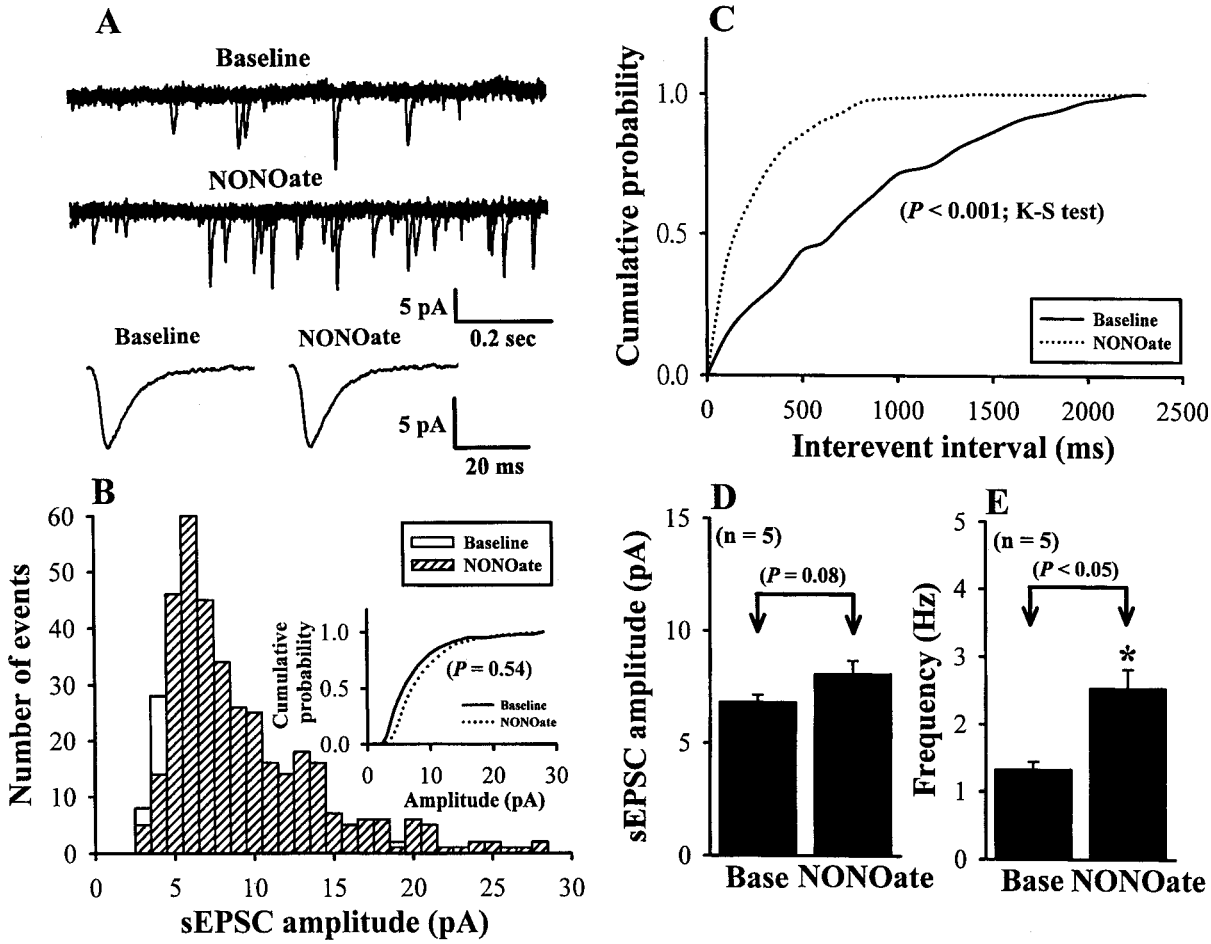

Fig. 7. Effects of spermine NONOate on the glutamatergic sEPSCs. A, sample traces (five traces superimposed) of sEPSCs before and after application of 100 μM spermine NONOate. Lower traces are the averaged sEPSCs of 30 events each before and after spermine NONOate (100 μM) application with increasing time resolution, demonstrating the lack of effect on the amplitude and kinetics of sEPSCs. B, amplitude histograms of sEPSCs. The threshold for peak detection was set at −3 pA. Data were binned in 1-pA intervals. Inset, cumulative probability plots of sEPSCs before (solid line) and during (dash line) application of spermine NONOate ($p = 0.54$; Kolmogorov-Smirnov test). C, cumulative interevent interval distribution illustrating a significant decrease in the interevent interval (i.e., increased frequency; $p < 0.001$; Kolmogorov-Smirnov test) during spermine NONOate application. D, summary of the effect of 100 μM spermine NONOate on the average amplitude and frequency of sEPSCs ($n = 5$). Data are presented as means ± S.E.M. *, $p < 0.05$ compared with the control baseline; Student's unpaired t test. The data shown in A, B, and C were taken from the same cell. Holding potential, −70 mV.

alone reduced both the amplitude and frequency of sEPSCs. Amplitude histograms show that TTX caused a reduction in the relative frequency of large-amplitude synaptic events. Additionally, TTX also reduce the relative frequency of large-amplitude synaptic events compared with control base (data not shown). Figure 8 illustrates that application of spermine NONOate (100 μM) also led to a significant increase in the frequency of mEPSCs. In five cells tested, spermine NONOate (100 μM) markedly increased the mean frequency of the sEPSCs from 0.62 $\pm$ 0.14 to 1.08 $\pm$ 0.15 Hz ($p < 0.05$; paired Student's t test) (Fig. 8, A and E). Significant differences in cumulative interevent interval distributions were observed in all five cells tested during spermine NONOate application; i.e., spermine NONOate shifted the interevent interval distribution of mEPSCs to shorter intervals ($p < 0.01$; Kolmogorov-Smirnov test). A typical example of recorded cell is shown in Fig. 8C. However, there was no significant effect of spermine NONOate (100 μM) on the mEPSC amplitude. This can be observed by a lack of effect of spermine NONOate on either the amplitude histogram (Fig. 8B) or the cumulative probability plots (Fig. 8B, inset; $p = 0.94$; Kolmogorov-Smirnov test). The mean amplitude of mEPSCs recorded in the presence of spermine NONOate (100 μM) was 6.63 $\pm$ 0.35 pA, which was of an amplitude comparable with that of mEPSCs recorded under control condition (6.19 $\pm$ 0.28 pA; $p > 0.05$; paired Student's t test). Therefore, these data further suggest that NO may act presynaptically to enhance the amount of glutamate release without changing the postsynaptic sensitivity to glutamate.

N-Type Ca^{2+} Channels Contribute to the Spermine NONOate-Induced Synaptic Potentiation. In a final series of experiments, we examined the possibility that NO modulates evoked EPSCs through an action on presynaptic voltage-sensitive Ca^{2+} channels, which contribute to supporting glutamate release. If spermine NONOate acts on presynaptic Ca^{2+} channels to affect glutamate release mechanisms, it would do so through one or more channel subtypes. We therefore examined the effect of spermine NONOate on the amplitude of EPSC before and after selective blockade of each of Ca^{2+} channel subtypes. We first examined the possible contribution of N-type Ca^{2+} channel enhancement to spermine NONOate-induced synaptic potentiation. A repre-

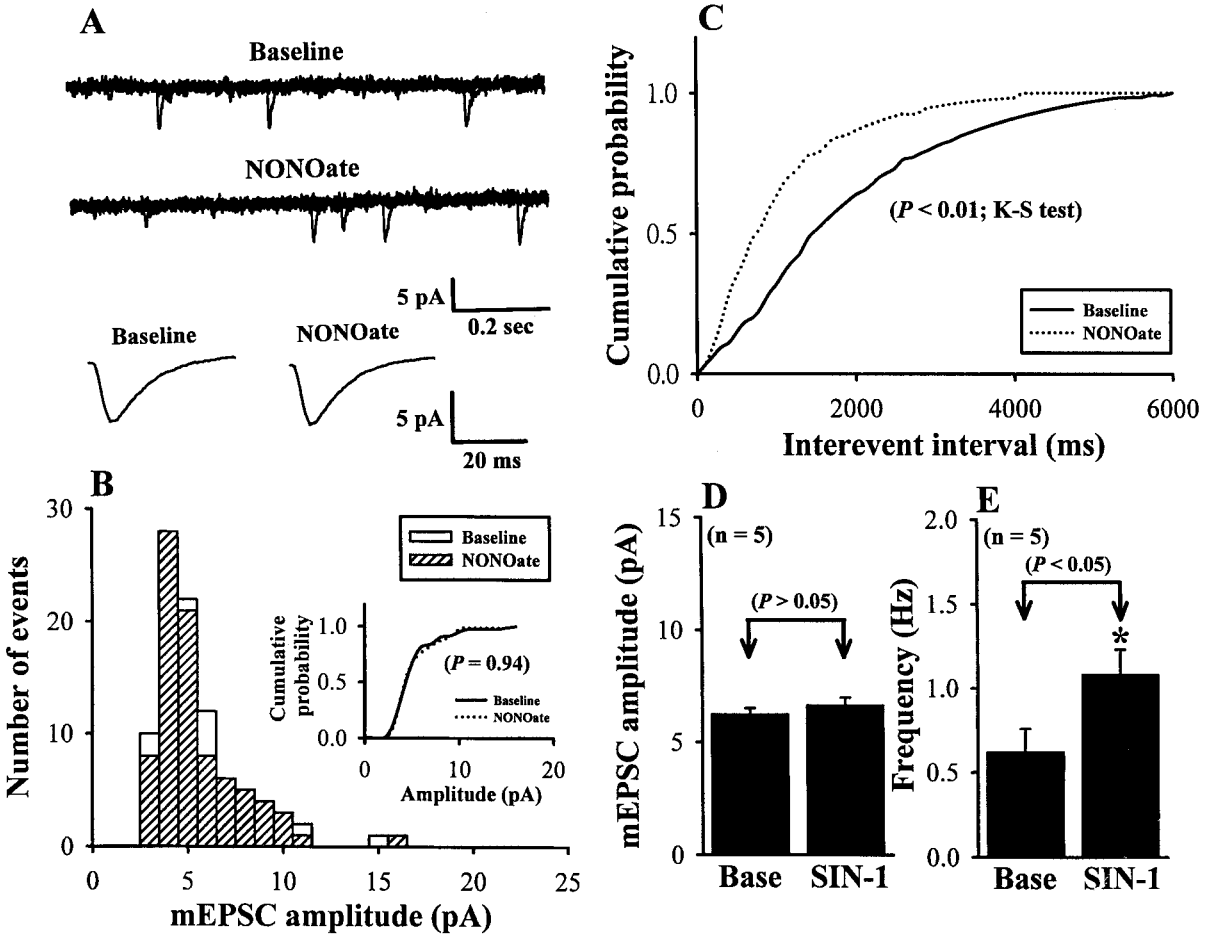

Fig. 8. Effects of spermine NONOate on the action potential-independent (TTX-resistant) mEPSCs. A, sample traces (five traces superimposed) of mEPSCs before (baseline: in the presence of 1 μM TTX to block Na^+ channels) and after application of 100 μM spermine NONOate. Lower traces are the averaged mEPSCs of 30 events each before and after spermine NONOate (100 μM) application with increasing time resolution, demonstrating the lack of effect on the amplitude and kinetics of mEPSCs. B, amplitude histograms of mEPSCs. The threshold for peak detection was set at -3 pA. Data were binned in 1 pA intervals. Inset, cumulative probability plots of mEPSCs before (solid line) and during (dashed line) application of spermine NONOate ($p = 0.94$; Kolmogorov-Smirnov test). C, cumulative interevent interval distribution illustrating a significant decrease in the interevent interval (i.e., increased frequency; $p < 0.01$; Kolmogorov-Smirnov test) during spermine NONOate application. D, summary of the effect of 100 μM spermine NONOate on the average amplitude and frequency of mEPSCs ($n = 5$). Data are presented as means $\pm$ S.E.M. *, $p < 0.05$ compared with the control baseline; Student's unpaired t test. The data shown in A, B, and C were taken from the same cell. Holding potential, -70 mV.

sentative cell recorded under this condition is shown in Fig. 9A. Application of ω-conotoxin-GVIA 1 μM, a concentration that should selectively block N-type Ca^{2+} channels (Kasai et al., 1987), caused a rapid, robust, and irreversible suppression of the amplitude of EPSCs by 72% and completely blocked the spermine NONOate action. In six neurons tested, spermine NONOate (100 μM) produced a 5.2 ± 3.6% increase in the amplitude of EPSCs after the application of ω-cono-

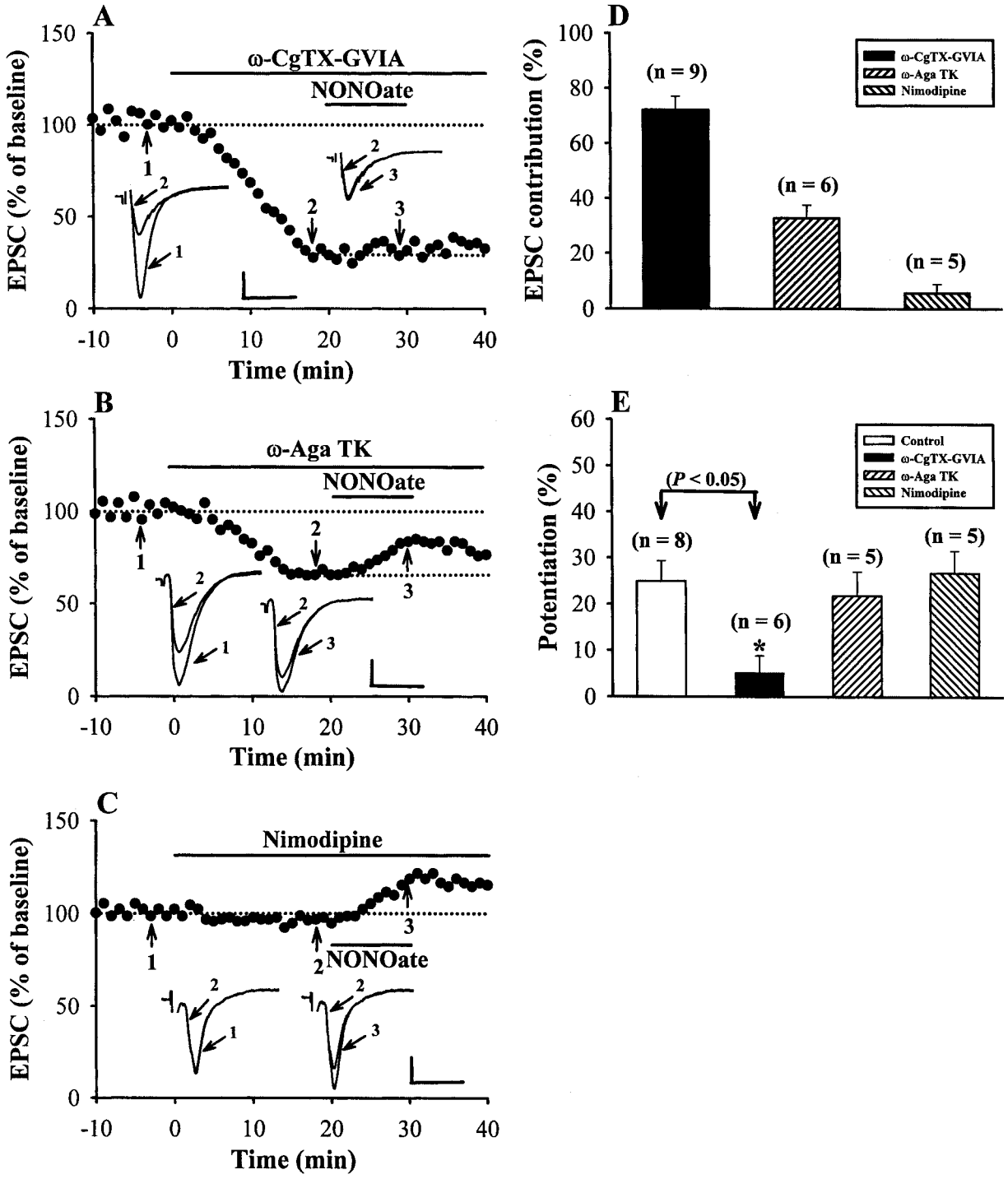

Fig. 9. The spermine NONOate-induced synaptic potentiation requires N-type Ca^{2+} channel modulation. A, a typical experiment in which the slice was perfused with 1 μM ω-conotoxin GVIA (ω-CgTX GVIA), which blocked ~72% of the EPSCs. It is clear that spermine NONOate (100 μM) failed to affect the fraction of synaptic responses insensitive to ω-CgTX GVIA. B, a typical experiment in which the slice was perfused with 200 nM ω-Aga TK, which blocked ~32% of the EPSCs. The fraction of EPSCs insensitive to ω-Aga TK was still sensitive to spermine NONOate. C, a typical experiment showing the effects of nimodipine (20 μM) on the EPSCs and spermine NONOate-induced synaptic potentiation. In this cell, nimodipine affected neither the basal synaptic transmission nor the action of spermine NONOate. D, summary histogram for all of the experiments performed as above with specific blocker of N-type (ω-CgTX GVIA; 1 μM), P/Q-type (ω-Aga TK; 200 nM), and L-type (nimodipine; 20 μM). The histogram of the maximum inhibitions caused by perfusion of selective agents reveals how the different types of voltage-sensitive Ca^{2+} channels contribute to the evoked EPSCs on the RVLM neurons. E, summary of the maximum 100 μM spermine NONOate-induced synaptic potentiation in the presence of Ca^{2+} channel blockers. Calibration bars: vertical, 50 pA; horizontal, 20 ms. *, $p < 0.05$; Student's unpaired t test.

toxin-GVIA, which was significantly different from that produced by spermine NONOate alone (22.5 ± 4.3%, $n = 8$; $p < 0.05$; unpaired Student's t test) (Fig. 9E).

We next investigated the role of P/Q-type Ca^{2+} channels in the modulation caused by spermine NONOate. ω-Aga-TK, a toxin purified from the venom of funnel web spider, was used in these experiments. ω-Aga-TK has been reported to selectively block the P-type Ca^{2+} channel at nanomolar concentrations, whereas at concentration >100 nM, it blocks not only P-type but also Q-type Ca^{2+} channels (Wheeler et al., 1994). As a representative experiment shown in Fig. 9B, application of 200 nM ω-Aga-TK reduced the amplitude of EPSCs by 32% compared with baseline. After the application of ω-Aga-TK, bath application of spermine NONOate (100 μM) for 10 min was still able to potentiate the residual EPSC amplitude by 21.8 ± 5.2% compared with baseline ($n = 5$), which was not significantly different from the synaptic potentiation produced by spermine NONOate alone (22.5 ± 4.3%, $n = 8$; $p > 0.05$; unpaired Student's t test) (Fig. 9E).

We further examined the possible contribution of L-type Ca^{2+} channel enhancement to spermine NONOate-induced synaptic potentiation. As a representative experiment shown in Fig. 9C, pretreatment of the slices with the selective L-type Ca^{2+} channel blocker nimodipine (20 μM) affected neither the basal EPSC amplitude nor the spermine NONOate-induced synaptic potentiation. In five neurons tested, spermine NONOate (100 μM) produced a 26.7 ± 4.8% increase in the amplitude of EPSCs after the application of nimodipine, which was not significantly different from that produced by spermine NONOate alone (22.5 ± 4.3%, $n = 8$; $p > 0.05$; unpaired Student's t test) (Fig. 9E). The conclusion from this series of experiments is that spermine NONOate-induced enhancement of glutamatergic synaptic transmission on the RVLM neurons is most likely through an increase the activity of presynaptic N-type but not P/Q-type or L-type Ca^{2+} channel subtypes.

Discussion

The present study demonstrates for the first time that NO enhances glutamatergic transmission in immature rat RVLM neurons from brainstem slices. This action involves activation of sGC and an increase in intracellular levels of cGMP, followed by activation of PKG to modulate presynaptic N-type Ca^{2+} channel activity.

Concerning the locus of NO-induced synaptic potentiation, a presynaptic site of action seems to be involved. We can give three lines of evidence to support this conclusion. First, the NO donor spermine NONOate produces a significant decrease in the failure rate of single-fiber EPSCs evoked by minimal stimulation (Fig. 6, A and B). Second, an increase in synaptic transmission by spermine NONOate was accompanied by a decrease in the magnitude of PPF ratio of synaptically evoked responses (Fig. 6C), which is usually considered an indication of a presynaptic mode of drug actions (Zucker, 1989). Third, and most importantly, spermine NONOate significantly increases the frequency of both sEPSCs and mEPSCs but did not affect their amplitude (Fig. 7 and 8). A change in the amplitude of sEPSCs and mEPSCs is usually interpreted as a postsynaptic modification, whereas a change in their frequency is typically associated with mechanisms that increase the probability of nerve-evoked transmitter release (Katz, 1969). Thus, the lack of effect of spermine NONOate on the amplitude of sEPSCs and mEPSCs also implies that the modulation of synaptic transmission by NO on the RVLM neurons is not mediated by a change in postsynaptic sensitivity to glutamate.

NO has been shown to activate several signal transduction pathways, including sGC, to increase cGMP levels (Garthwaite, 1991). The involvement of NO/cGMP pathway in the modulation of glutamatergic transmission has been demonstrated in slice preparations from the hippocampus (O'Dell et al., 1991; Boulton et al., 1994) and locus ceruleus (Pineda et al., 1996) and in cultured hippocampal neurons (Arancio et al., 1995). In the present results, both L-arginine and NO donor-induced synaptic potentiation were prevented by a selective NO-sensitive sGC inhibitor, ODQ (Fig. 4). It is likely that NO is acting through a NO-sensitive sGC/cGMP signaling pathway to increase glutamatergic transmission on the RVLM neurons. Various potential mechanisms can account for the cellular function of cGMP in different systems. The specific targets for cGMP are PKG (Paupardin-Tritsch et al., 1986), cyclic nucleotide-gated cationic channels (Fesenko et al., 1985), and cyclic nucleotide-stimulated and -inhibited phosphodiesterases (Nicholson et al., 1991). In the present study, experiments were performed with activator (8-pCPT-cGMP) or inhibitor (*R*p-8-Br-cGMPS) of PKG to characterize the pathway involved in NO effect. The experiments showed that preincubation of the slices with *R*p-8-Br-cGMPS fully prevented SIN-1- and spermine NONOate-induced synaptic potentiation (Fig. 5, A and B), whereas bath application of 8-pCPT-cGMP mimicked the action of NO donors (Fig. 5C). In addition, both 8-pCPT-cGMP and *R*p-8-Br-cGMPS have a negligible activity on cyclic nucleotide-stimulated and -inhibited phosphodiesterases, indicating that the activation of cyclic-nucleotide phosphodiesterases is not necessary for the NO-induced synaptic potentiation. Therefore, our results support the idea that NO-induced synaptic potentiation on the RVLM neurons is mediated via a cGMP/PKG-coupled signaling pathway. However, we could not exclude the possibility that the increase in cGMP levels by NO-stimulated sGC may directly modulate presynaptic cyclic nucleotide-gated cationic channels, which leads to depolarization of the presynaptic terminals; potentiation of transmitter release may also play a part role in the NO-induced synaptic potentiation (Ludwig et al., 1998).

What is the biological step downstream of cGMP/PKG responsible for the NO-induced synaptic potentiation? The most likely candidate is their facilitatory coupling with presynaptic voltage-sensitive Ca^{2+} channels, which in turn enhances glutamate release. Various subtypes of voltage-sensitive Ca^{2+} channels are known to be involved in neurotransmitter release. In the present study, by using the highly selective inhibitors of voltage-sensitive Ca^{2+} channels, distinct subtypes of voltage-sensitive Ca^{2+} channels contributing to the evoked release of glutamate on the RVLM neurons were identified. Data reported in this article represent the first experimental evidence that N- and P/Q-type Ca^{2+} channels make the major contribution to the evoked glutamate release in the RVLM area (Fig. 9D). The finding that spermine NONOate-induced synaptic potentiation dropped from 22 to 5% after exposure to the N-type Ca^{2+} channel blocker ω-CgTX GVIA (Fig. 9, A and D) is evidence that the enhancement of this channel activity is the primary

mechanism of NO-induced potentiation of glutamate release from presynaptic nerve terminals. In salamander retinal ganglion cells, a recent study also demonstrated that NO can enhance N-type Ca^{2+} channel activity by facilitating their voltage-dependent activation via a mechanism involving sGC/cGMP/PKG-dependent phosphorylation (Hirooka et al., 2000). The evidence that blockade of P/Q-type and L-type Ca^{2+} channels had no effect on the spermine NONOate-induced synaptic potentiation seems to rule out the involvement of these channel subtypes.

Our observation that spermine NONOate also enhances the frequency but not the amplitude of the mEPSCs suggests that NO has effect in addition to its modulation of voltage-sensitive Ca^{2+} channels. Because concentrations of Ca^{2+} channel blockers sufficient to abolish all evoked transmitter release have no effect on mEPSC frequency, changes in mEPSC frequency are not likely to be the result of changes in Ca^{2+} influx from voltage-sensitive Ca^{2+} channels at the resting membrane potentials (Scanziani et al., 1992). The NO-mediated increase in mEPSC frequency therefore may reflect a direct action on the exocytotic apparatus or protein kinase-dependent phosphorylation of targets that regulate the vesicle release machinery.

An important issue that arose in this study was whether the NO concentrations released from donor compounds could be reached under physiological or pathological conditions in the brain. Although the local NO concentrations in slice preparations produced by SIN-1 (200 μM) and spermine NONOate (100 μM) remain unknown, it has been demonstrated that spermine NONOate at a concentration of 82.7 μM will generate a peak NO concentration in the Tyrode's solution of 3 to 4 μM (Ramamurthi and Lewis, 1997). Moreover, tissue-derived factors may accelerate NO breakdown in slice studies, because NO decays more quickly when perfused over tissues compared with the experiments in tubes (Palmer et al., 1987). In a recent report, it was calculated that the concentrations of NO produced by another NO donor, 2,2-diethyl-1-nitroso-oxyhydrazine (100–300 μM), were in the 100 nM range in the hippocampal slices (Bon and Garthwaite, 2001). Hence, the local NO concentrations produced by 100 μM spermine NONOate in the present study should be in the 50 to 100 nM range. Because it is known that the physiological range of NO concentration in the brain is 10 to 100 nM and ischemic conditions produce NO of about 2 to 4 μM (Shibuki and Okada, 1991; Malinski and Taha, 1992), the NO-induced synaptic potentiation on the RVLM neurons described in the present study would be expected to occur in vivo under physiological or ischemic situations.

In conclusion, we here extended the earlier studies on the role of NO and glutamate in the RVLM, providing further evidence that NO may substantially enhance glutamatergic transmission on the RVLM neurons. Consisting of premotor sympathetic neurons, the RVLM is believed to maintain basal levels of systemic arterial pressure (Ross et al., 1984) by providing tonic excitation to preganglionic sympathetic neurons in the intermediolateral cell column of the spinal cord. The glutamatergic afferents to the RVLM control the premotor neurons, which in turn excite the preganglionic neurons in the spinal cord, which send their axons to the periphery and synapses with sympathetic postganglionic neurons. Via the increase in the excitatory synaptic transmission in the RVLM, NO could indirectly excite preganglionic neurons of the spinal cord, increasing their firing rate, and trigger sympathoexcitatory functions, such as increasing SAP and heart rate.

References

Arancio O, Kandel ER, and Hawkins RD (1995) Activity-dependent long-term enhancement of transmitter release by presynaptic 3′,5′-cyclic GMP in cultured hippocampal neurons. *Nature (Lond)* **376:**74–80.

Bon CL and Garthwaite J (2001) Exogenous nitric oxide causes potentiation of hippocampal synaptic transmission during low-frequency stimulation via the endogenous nitric oxide-cGMP pathway. *Eur J Neurosci* **14:**585–594.

Boulton CL, Irving AJ, Southam E, Potier B, Garthwaite J, and Collingridge GL (1994) The nitric oxide-cyclic GMP pathway and synaptic depression in rat hippocampal slices. *Eur J Neurosci* **6:**1528–1535.

Chan SHH, Wang LL, Wang SH, and Chan JYH (2001) Differential cardiovascular responses to blockade of nNOS or iNOS in rostral ventrolateral medulla of the rat. *Br J Pharmacol* **133:**606–614.

Chang AYM, Chan JYH, Kao FJ, Huang CM, and Chan SHH (2001) Engagement of inducible nitric oxide synthase at the rostral ventrolateral medulla during mevinphos intoxication in the rat. *J Biomed Sci* **8:**475–483.

Dampney RA (1994) The subretrofacial vasomotor nucleus: anatomical, chemical and pharmacological properties and role in cardiovascular regulation. *Prog Neurobiol* **42:**197–227.

Deuchars SA, Morrison SF, and Gilbey MP (1995) Medullary-evoked EPSPs in neonatal rat sympathetic preganglionic neurones in vitro. *J Physiol* **487:**453–463.

Fesenko EE, Kolesnikov SS, and Lyubarsky AL (1985) Induction by cyclic GMP of cationic conductance in plasma membrane of retinal rod outer segment. *Nature (Lond)* **313:**310–313.

Garthwaite J (1991) Glutamate, nitric oxide and cell-cell signalling in the nervous system. *Trends Neurosci* **14:**60–67.

Guyenet PG, Koshiya N, Huangfu D, Baraban SC, Stornetta RL, and Li YW (1996) Role of medulla oblongata in generation of sympathetic and vagal outflows. *Prog Brain Res* **107:**127–144.

Hakim MA, Hirooka Y, Coleman MJ, Bennett MR, and Dampney RA (1995) Evidence for a critical role of nitric oxide in the tonic excitation of rabbit renal sympathetic preganglionic neurons. *J Physiol* **482:**401–407.

Hirooka K, Kourennyi DE, and Barnes S (2000) Calcium channel activation facilitated by nitric oxide in retinal ganglion cells. *J Neurophysiol* **83:**198–206.

Hirooka Y, Polson JW, and Dampney RA (1996) Pressor and sympathoexcitatory effects of nitric oxide in the rostral ventrolateral medulla. *J Hypertens* **14:**1317–1324.

Holm P, Kankaanranta H, Metsa-Ketela T, and Moilanen E (1998) Radical releasing properties of nitric oxide donors GEA 3162, SIN-1, and *S*-nitroso-*N*-acetylpenicillamine. *Eur J Pharmacol* **346:**97–102.

Huang CC, Lo SW, and Hsu KS (2001) Presynaptic mechanisms underlying cannabinoid inhibition of excitatory synaptic transmission in rat striatal neurons. *J Physiol* **532:**731–748.

Hwang LL and Dun NJ (1998) 5-Hydroxytryptamine responses in immature rat rostral ventrolateral medulla neurons in vitro. *J Neurophysiol* **80:**1033–1041.

Ignarro LJ (1991) Signal transduction mechanisms involving nitric oxide. *Biochem Pharmacol* **41:**485–490.

Kagiyama S, Tsuchihashi T, Abe I, and Fujishima M (1997) Cardiovascular effects of nitric oxide in the rostral ventrolateral medulla of rats. *Brain Res* **757:**155–158.

Kasai H, Aosaki T, and Fukuda J (1987) Presynaptic Ca-antagonist omega-conotoxin irreversibly blocks N-type Ca-channels in chick sensory neurons. *Neurosci Res* **4:**228–235.

Katz B (1969) *The Release of Neural Transmitter Substances*. Liverpool University Press, Liverpool, UK.

Ludwig A, Zong X, Jeglitsch M, Hofmann F, and Biel M (1998) A family of hyperpolarization-activated mammalian cation channels. *Nature (Lond)* **393:**587–591.

O'Dell TJ, Hawkins RD, Kandel ER, and Arancio O (1991) Tests of the roles of two diffusible substances in long-term potentiation: evidence for nitric oxide as a possible early retrograde messenger. *Proc Natl Acad Sci USA* **88:**11285–11289.

Malinski T and Taha Z (1992) Nitric oxide release from a single cell measured in situ by a porphyrinic-based microsensor. *Nature (Lond)* **358:**676–678.

Morrison SF, Callaway J, Milner TA, and Reis DJ (1991) Rostral ventrolateral medulla: a source of the glutamatergic innervation of the sympathetic intermediolateral nucleus. *Brain Res* **562:**126–135.

Mtui EP, Anwar M, Reis DJ, and Ruggiero DA (1995) Medullary visceral reflex circuits: local afferents to nucleus tractus solitarii synthesize catecholamines and project to thoracic spinal cord. *J Comp Neurol* **351:**5–26.

Nicholson CD, Challiss RA, and Shahid M (1991) Differential modulation of tissue function and therapeutic potential of selective inhibitors of cyclic nucleotide phosphodiesterase isoenzymes. *Trends Pharmacol Sci* **12:**19–27.

Palmer RMJ, Ferrige AG, and Moncada S (1987) Nitric oxide release accounts for the biological activity of endothelium-derived relaxing factor. *Nature (Lond)* **327:**524–526.

Paupardin-Tritsch D, Hammond C, Gerschenfeld HM, Nairn AC, and Greengard P (1986) cGMP-dependent protein kinase enhances Ca^{2+} current and potentiates the serotonin-induced Ca^{2+} current increase in snail neurons. *Nature (Lond)* **323:**812–814.

Pineda J, Kogan JH, and Aghajanian GK (1996) Nitric oxide and carbon monoxide activate locus coeruleus neurons through a cGMP-dependent protein kinase: involvement of a nonselective cationic channel. *J Neurosci* **16:**1389–1399.

Raastad M (1995) Extracellular activation of unitary excitatory synapses between hippocampal CA3 and CA1 pyramidal cells. *Eur J Neurosci* **7:**1882–1888.

Ramamurthi A and Lewis RS (1997) Measurement and modeling of nitric oxide release rates for nitric oxide donors. *Chem Res Toxicol* **10:**408–413.

Ross CA, Ruggiero DA, Park DH, Joh TH, Sved AF, Fernandez-Pardal J, Saavedra JM, and Reis DJ (1984) Tonic vasomotor control by the rostral ventrolateral medulla: effect of electrical or chemical stimulation of the area containing C_1 adrenaline neurons on arterial pressure, heart rate and plasma catecholamines and vasopressin. *J Neurosci* **4:**474–494.

Scanziani M, Capogna M, Gahwiler BH, and Thompson SM (1992) Presynaptic inhibition of miniature excitatory synaptic currents by baclofen and adenosine in the hippocampus. *Neuron* **9:**919–927.

Shibuki K and Okada D (1991) Endogenous nitric oxide release required for long-term synaptic depression in the cerebellum. *Nature (Lond)* **349:**326–328.

Stevens CF and Wang Y (1994) Changes in reliability of synaptic function as a mechanism for plasticity. *Nature (Lond)* **371:**704–707.

Sved AF, Ito S, Madden CJ, Stocker SD, and Yajima Y (2001) Excitatory inputs to the RVLM in the context of the baroreceptor reflex. *Ann NY Acad Sci* **940:**247–258.

Trackey JL, Uliasz TF, and Hewett SJ (2001) SIN-1-induced cytotoxicity in mixed cortical cell culture: peroxynitrite-dependent and -independent induction of excitotoxic cell death. *J Neurochem* **79:**445–455.

Vincent SR and Kimura H (1992) Histochemical mapping of nitric oxide synthase in the rat brain. *Neuroscience* **46:**755–784.

Wheeler DB, Randall A, and Tsien RW (1994) Roles of N-type and Q-type Ca^{2+} channels in supporting hippocampal synaptic transmission. *Science (Wash DC)* **264:**101–111.

Zanzinger J, Czachurski J and Seller H (1995) Inhibition of basal and reflex-mediated sympathetic activity in the RVLM by nitric oxide. *Am J Physiol* **268:** R958–R962

Zucker RS (1989) Short-term synaptic plasticity. *Annu Rev Neurosci* **12:**13–31.

Address correspondence to: Dr. Kuei-Sen Hsu, Department of Pharmacology, College of Medicine, National Cheng Kung University, 1, Ta-Hsiue Rd., Tainan 701, Taiwan. E-mail: richard@mail.ncku.edu.tw